

Theoretical investigation of one -dimensional cavities in two dimensional photonic crystals

S. Foteinopoulou ¹ and C.M. Soukoulis ^{1,2}

¹Ames Laboratory-USDOE and Department of Physics and Astronomy
Iowa State University, Ames, Iowa 50011

²Research Center of Crete-FORTH and Department of Physics,
University of Crete, Heraklion, Crete 71110, Greece

We study the features of the resonant peak of one dimensional (1D) dielectric cavities in a two-dimensional (2D) hexagonal lattice. We use both the transfer matrix method and the finite difference time domain (FDTD) method to calculate the transmission coefficient. The results of the two methods are compared and discussed. The Q factor of the 1D cavities is numerically obtained and agrees reasonably well with the experimental results. The dependence of Q on absorption and losses, the thickness of the sample and the lateral width of the cavity is examined. It's dependence on the width of the source in the FDTD calculations is given. The agreement between experiments and numerics is very good, provided that either the source in the FDTD is narrow or an imaginary part (in the air dielectric) is introduced in the transfer matrix calculation.

I. INTRODUCTION

In semiconductor crystals the presence of the periodic potential affects the properties of the electrons. Likewise in photonic crystals (PC's), that are periodic dielectric arrangements in one, two or three dimensions the properties of the photon can be controlled. For certain frequency regions known as "the photonic band gap" propagation of electromagnetic (EM) waves is prohibited in the photonic crystal¹⁻³. A defect present in an otherwise periodic crystal may introduce one or more propagation modes in the band gap and forms a cavity. Cavities of different geometries can exist in a photonic crystal and the resulting resonant mode can be classified into two general types indicating whether it drops from the "air" (higher) band or raises from the "dielectric" (lower) band⁴. The first type is associated with defects corresponding to removal of dielectric material while the second corresponds to defects involving addition of dielectric material. The features of the resonant mode will depend on both the bulk crystal and the cavity characteristics and can so be tuned accordingly^{1,2,4}.

An important virtue of the PC cavity is that it can control the atomic spontaneous emission, while metallic cavities for the related frequency range are generally lossy⁵⁻⁷. Spontaneous emission is important for a number of semiconductor devices⁸. Resonant cavities have undergone extensive studies^{7,9-12}, both theoretical and experimental. A variety of applications incorporating a PC cavity have been suggested or reported^{13,14}, such as optical laser components^{1,2}, optical filters⁴, single mode light emitting diode (SMLED)^{8,15}, optical imaging¹⁶ e.t.c.

In this paper we focus on the theoretical study of 1D dielectric cavity in between a hexagonal patterned region of air cylinders in a dielectric matrix for the case of H polarization (magnetic field along the cylinder axis). We

will present the cavity mode frequency versus the cavity length (L_c) (see fig. 1), as well as the quality factor (Q) of the modes versus their corresponding frequency. The quality factor is defined as $\lambda_p/\delta\lambda$ where λ_p the frequency of the resonant peak and $\delta\lambda$ the width of the resonance at transmission half of its maximum value. The dependence of the resonant mode on the size of the system (in the lateral direction and in the direction of propagation) will be also shown. In our calculations two different numerical techniques (the transfer matrix and the FDTD) are used and the results of the two methods are compared and discussed. With both techniques we calculate the transmission through the structure and from that we obtain all the relevant features of the resonant mode. Finally we will compare our results with the experimental ones previously performed on the structure under study¹⁷.

In section 2 we describe briefly the two calculational methods. In section 3 we present and discuss our calculational results concerning the quality factor and position of the cavity resonance and compare them with the experiment. In section 4 we give a summary of our results.

II. CALCULATIONAL METHODS

The first technique we use is the transfer matrix method (TMM) developed by Pendry^{18,19}. In the TMM a grid lattice is used to discretize the space, and the structure is divided into finite blocks along the propagation direction. With the use of the Maxwell's equations, - that are solved on the grid lattice -, the electric and magnetic field can be integrated throughout the blocks and so the respective transmission coefficient can be calculated. The final transmission will result by combining the ones of the individual blocks. In the transfer matrix method the

modeled structure is finite in the propagation direction (y) but infinite in the x,z (where z is the direction of the air cylinders), and the incoming EM wave is a plane wave. The structure is embedded in a medium with dielectric constant equal to the background dielectric constant to simulate the experiment.

The second method we use is the finite difference time domain (FDTD) technique^{20,21}. The real space is discretized on a grid lattice and Maxwell's equations are solved in time domain. The electric and magnetic fields get updated in every point of the grid lattice in finite time steps. The structure is infinite in the direction of the cylinders (z directions) but has finite size in both x and y direction and is embedded in a finite sized (in x and y) dielectric slab with dielectric constant equal to that of the matrix medium. Liao absorbing boundary conditions²² are applied at the walls of the slab to avoid reflections. The source is located close to $x=0$, $y=0$ (y being the direction of propagation), has finite length and generates fields with extended (with gaussian tails) profile in space.

III. RESULTS

In Fig. 1 the cross section of the cavity structure under study with the x-y plane can be seen. It corresponds to air cylinders ($\epsilon_a = 1.0$) in a GaAs background ($\epsilon_b = 11.3$) (the value of the GaAs dielectric constant for 1000 nm is taken in the calculations for simplicity). The symmetry directions of the bulk crystal are also shown. With L_c we will refer to the cavity width that corresponds to the length of the dielectric defect introduced along the propagation direction. With L_w we will refer to the latteral width of the cavity (which is the same as the sample's latteral width). N_c will be the number of rows in each side of the cavity ($N_c = 4$ for both calculations and experiment). The thickness of the sample then along the propagation direction would be $L_{th} = 2N_c b + L_c$, where $2b = \sqrt{3}a$ (but is approximated with 1.7a in the TMM for numerical reasons). The radius R of the air holes is $R \sim 0.2803a$ (a being the lattice constant) that corresponds to a filling factor of ~ 0.285 . (Actually in the TMM because of the approximation mentioned above the simulated structure will have a slightly larger filling factor). No specific value for the lattice constant a is assumed. All the band gap and transmission properties in a photonic crystal scale with the lattice constant a so all the subsequent results will be presented in dimensionless units of frequency (reduced frequency $u = a/\lambda$) and length.

From the transfer matrix results for the various L_c we observed that the spectral gap when the cavity is introduced is wider than the one for the periodic crystal. Widening of the gap but for the case when an air defect is introduced in a periodic system of dielectric rods in air background has been observed also in the past¹². Another interesting observation is that both the trans-

mission around the gap edges for the periodic system and the one of the resonant peak for the cavity structure do depend not only on the values of the constituents dielectrics but also on the dielectric constant of the medium that the whole structure is embedded in. This can be clearly seen in Fig. 2. In Fig. 2a the transmission for the periodic crystal for two different embedding media (air and GaAs ($\epsilon = 11.3$)) is shown. In Figures 2b and 2c three cavity resonances are shown for air and GaAs as the embedding medium respectively. It can be clearly seen that for the second case (where the embedding medium and background dielectric are the same) the transmission is always around one while the corresponding peaks with air as the embedding medium can have transmission much smaller than one and are also characterized by smaller quality factor values. However the position of the peaks is almost the same for both embedding media. All the following TMM and FDTD calculations are performed with GaAs as the embedding medium which is the case of the experiment. TMM calculation have been performed for various cavity structures with dimensionless L_c/a ranging from 0.15 to 2.0. At a certain frequency different resonances (peaks) can occur corresponding to different L_c values. Each of these peaks is characterized by an order, that basically indicates the order at which a resonant peak appears at this specific frequency while L_c is increasing. In Figures 2b and 2c the three peaks depicted for $L_c/a = 0.535, 1, 1.335$ are 1st, 2nd and 3rd order respectively.

In Fig. 3 every cavity width (in units of a) is plotted as a function of the corresponding reduced frequency of the observed peak and three different curves are recovered for the three orders of the resonant peaks. Starting from the lower to the higher curve in Fig. 3 the peaks are the 1st, 2nd and 3rd order respectively. It will be seen later that peaks of the same frequency but different order can have different features (e.g. quality factor). It is evident from Fig. 3 that for certain L_c values more than one resonant peaks can appear within the gap. The experimental results¹⁷ for the resonant peaks for various lattice constants ($a = 200$ nm, 210nm, 220nm, 230nm, 240nm) are also included in the figure. The agreement is generally good but there seems to be a small discrepancy that increases with the frequency. This can be attributed to the fact that we have taken the GaAs dielectric constant not to vary with the frequency (for simplicity the value at 1000 nm is taken in our calculations) while this is not the case in the actual system. This difference in the dielectric will alter slightly the position of the peaks¹⁷. This is consistent with the fact that the discrepancy at the higher end of the reduced frequencies seems to be a little larger for the smaller lattice constant (the corresponding wavelength differs more from the value of a 1000 nm). There are also some experimental peaks for $a = 200$ nm that are falling above the theoretical curves as for example the 1st order peaks with L_c/a from ~ 0.60 to 0.85. Due to the set-up in the experimet only peaks that fall in the wavelength range of ~ 920 nm to 1100 nm can

be determined accurately. For the cases mentioned above the 2nd order peaks that appear in the gap do not fall in that wavelength range. Therefore only the 1st order lower frequency ones are recorded. We have not numerically calculated the Q's for these because they lie too close to the band edges and the determination of their quality factor can be vague and so we have not included them in Fig. 3.

We compare now the two computational methods (TMM and FDTD) that are used to simulate the experiment. There are basically three fundamental differences between the two methods. The first one is that the transfer matrix technique is a time independent method while in the FDTD the fields are solved in time domain. Also in the TMM the structure is infinite in x by virtue of the periodic boundary conditions applied along this direction, while in the FDTD the system is finite in the x-y plane bounded by absorbing boundary conditions. Finally, the incoming EM fields in the TMM are extended plane waves incident on the whole x-z boundary (corresponding to a source infinite in width) while in the FDTD a pulse emitted from a source with finite width is considered. In order to make the comparison between the two methods in this particular FDTD calculation the 2D space is discretized as in transfer matrix which gives $2b=1.7 a$ instead of $\sqrt{3} a$. The results for one particular cavity width are shown in Fig. 4. A very good agreement is found between the two methods regarding the positions of the resonant peak and the band gap edges but there is a discrepancy in the quality factor of the peak, that can be possibly attributed to the differences between the two methods mentioned above.

It is interesting therefore to see how the quality factor of the resonant peak is affected by the finiteness of the size of the system and the width of the source, in our FDTD calculations. This can be seen in Fig. 5a and 5b where the quality factor versus the latteral width of the sample (L_w) and versus the source width are shown respectively. In Fig. 5a the ratio of the source width over the latteral extent of the structure L_w (defined in Fig. 1) is kept constant (equal to 0.5). It can be seen that as the latteral width approaches $20a$, Q saturates at a value of ~ 160 which is still considerably smaller than the value of ~ 210 obtained by the TMM. TMM values calculated using a small imaginary part in the dielectric constant of the cylinder holes are also shown in Fig. 5a. The dielectric part is introduced to model various losses out of the plane of periodicity¹⁷ that are present in the real structure. In Fig. 5b we present results of the Q versus the source width for a system with a latteral width of $L_w = 40a$. The width L_w is large enough for the quality factor to have reached its saturation value (that is related to the latteral size) so that one can see the dependence on the source width only. It is clearly seen that for a small source width the quality factor drops significantly. Experimental data for values of L_c/b close to the one of the modeled structure are also shown in Fig. 5b as horizontal lines for comparison. It can be therefore

argued that the finiteness of the system in the lateral direction as well as the finite source width can reduce the quality factor. This reduction can be also achieved by introducing imaginary parts with values of 0.02-0.05 in the air dielectric constant in the TMM system. The latter has been suggested in ref. 17 as a mechanism to model out of plane losses.

Fig. 6a shows the transmission calculated with the TMM method versus the reduced frequency $u=a/\lambda$ for a 1D cavity of width $L_c/a=0.985$ and $N_c=4$, for different imaginary parts in the air dielectric constant. N_c is the number of rows of air cylinders in each side of the 1D dielectric cavity. As expected the transmission peak decreases with $\text{Im } \epsilon$ while the width of the transmission increases with $\text{Im } \epsilon$. We have also examined how the size of the system along the propagation direction affects the characteristics of the resonance. In Fig. 6b the dimensionless linewidth Δ/a - which is defined as $\delta\lambda/a$ (where $\delta\lambda$ is the width in wavelength of the resonance at the half maximum value) - is plotted versus N_c (the number of rows of cylinders on each side of the dielectric cavity) in semi-logarithmic scale. As mentioned previously N_c is related with the thickness of the system L_{th} through the relation $L_{th} = 2N_c b + L_c$ (L_{th} is shown in Fig. 1) A linear relation in the semi-log scale between Δ/a with N_c is obtained, meaning that the quality factor Q, which is inversely proportional to Δ/a would increase exponentially with N_c . That is consistent with results for other defect cavities^{12,23}. In Sigalas et. al.¹², where an air defect in a dielectric array is studied, it was shown that when absorption is introduced in the dielectric the quality factor saturates and does not increase any further as the size of the system increases. Such saturation with the introduction of an imaginary part in the dielectric of the holes is observed in our case too as it can be seen in Fig. 6b. We also observe (as in ref. 12) that the saturation value of the linewidth Δ is smaller the larger the imaginary part in the dielectric.

In Fig. 7 we present the results done with the TMM of the transmision height versus N_c for 1D cavity of width $L_c/a=0.985$ for three different $\text{Im } \epsilon$ of the air dielectric. Notice that for $\text{Im } \epsilon=0.0$ the height is always one, i.e perfect transmision. However for non-zero $\text{Im } \epsilon$, the transmission height drops as N_c increases. Two experimental values are shown for almost the same width of L_c/a as the one in the calculations. Notice that this suggests that the $\text{Im } \epsilon$ that can fit the experimental data can have a value close to 0.04.

For the ideal case with no losses present the quality factor was calculated by the TMM for various cavity widths L_c that led to peaks that span most of the bandgap. In Fig. 8 the quality factor is plotted versus the reduced frequency of the peak. (Peaks too close to the edges of the bandgap were not used because the determination of their Q would be vague as stated earlier in this paper). For every frequency in the plot there are three peaks that are characterized by different order and correspond to different L_c values (see Fig. 3). So three

different curves are recovered when grouping the peaks according to order. Higher order peaks are characterized by a higher value of the quality factor. For every order the quality factor is maximum for a frequency close to the center of the band gap and reduces as the frequency approaches either edge of the band gap. The calculations above were performed with a grid lattice dividing the lattice constant a in 10 intervals. We have investigated the dependence of the quality factor with the accuracy of the TMM given by the number N of intervals the lattice constant is divided to, i.e. N is the number of grid points. It was done for three different peaks. One close to the band gap center and the others close to the lower and higher frequency band edge respectively. It is seen from Fig. 9 that the quality factor increases with increasing accuracy and eventually saturates at a value.

We will now compare the numerical results obtained by the two calculational methods with the experimental results. In order to do that the quality factor for various L_c is calculated with the FDTD method, only for the 2nd order peaks and with $L_w = 40a$ (corresponding to 40 sites along x). In the experiment the lateral extent of the structure corresponds to about 100 cells in the x direction. As we have argued previously when we discussed Fig. 5, if L_w is greater than $20a$ in the FDTD calculation, the results for Q are reliable. The source used in the experiment is a red laser diode that is focused on the sample¹⁷. Details of the optical setup are given also in ref. 24.

We do not attempt to make a quantitative correspondence between experiment and the FDTD results. We only qualitatively discuss how Q , that can be reduced when a small width source is used instead of an extended one, compares with the experiment. In the TMM a plane wave is incident on the structure which means that width of the source is infinite i.e. as big as the width of the structure. The source width was chosen to be $5a$ in the FDTD simulations. The results are shown in Fig. 10 where the second order peaks calculated from the TMM, from the FDTD with small source width, and the experimental ones are given. There is a large number of experimental data that fall very close to the FDTD curve and some that fall below. In the experiment the transmission of the peaks has also a value less than one, as in the numerical results shown in Fig. 7. Trully there are out of plane losses due to the finite size of the experimental sample in z direction¹⁷ (about 700 nm deep). But this might not be the main factor that accounts for the reduced Q . We argue that the smaller experimental Q values could stem from a combined effect of the following: losses out of the plane of periodicity, the finiteness of the structure in the lateral direction (x) and the use of a finite source width focusing on a small area of the sample.

IV. CONCLUSIONS

We have studied 1-D dielectric cavity structure in a 2d hexagonal array with the Transfer Matrix Method and the Finite Difference Time Domain method, and have compared our results with experiments performed in that structure¹⁷. There is very good agreement for the position of the defect peak between the theoretical methods and the experiment. The quality factor though shows sensitivity to a lot of parameters such as the size of the system (both lateral and along the propagation direction), the type of the incoming EM fields and losses out of the plane of periodicity. It was investigated how the quality factor varies with those parameters. In that context the discrepancy of the experimental quality factor with the theoretical values was discussed. Good agreement was found with the results from the FDTD method when using a small in width source for the incoming EM fields.

ACKNOWLEDGMENTS

We would like to acknowledge H. Benisty, M. Agio, M. Rattier and M. Sigalas for helpful discussions. Ames Laboratory is operated by the U.S Department of Energy by Iowa State University under Contract No. W-7405-Eng-82. This work is supported by the IST project PCIC of the European Union and the NSF grant INT-0001236.

-
- ¹ J. D. Joannopoulos, R. D. Meade, J. N. Winn , “Photonic Crystals: Molding the flow of light”, Princeton University Press, 1995.
- ² “Photonic Band Gap Materials”, ed. by C. M. Soukoulis (Kluwer, Dordrect, 1996).
- ³ P. R. Villeneuve and M. Piche, *Prog. Quant. Electr.* **18**, 153 (1994).
- ⁴ J.D. Joannopoulos in “Photonic Band Gap Materials” ed. by C. M. Soukoulis , NATO ASI SERIES E **315**, 1 (1996).
- ⁵ R. K. Lee, O. Painter, B. Kitzke, A. Scherer and A. Yariv *J. Opt. Soc. Am. B* **17**, 629 (2000).
- ⁶ N. M. Lawandy and Gyeong-il Kweon in “Photonic Band Gaps and Localization” ed. by C. M. Soukoulis , NATO ASI SERIES B **308**, 355 (1993).
- ⁷ S.-Y. Lin, V. M. Hietala, and S. K. Lyo and A. Zaslavsky, *Appl. Phys. Lett.* **68**, 3233 (1996).
- ⁸ E. Yablonovitch, *J. Mod. Opt.* **41**, 173 (1994).
- ⁹ C. J. M. Smith and T. F. Krauss and H. Benisty, M. Rattier and C. Weisbuch and U. Oesterle and R. Houdre *J. Opt. Soc. Am. B* **17**, 2043 (2000).
- ¹⁰ C. J. M. Smith and R.M. De La Rue and M. Rattier, S. Olivier, H. Benisty, and C. Weisbuch and T.F. Krauss and

- R. Houdre and U. Oesterle, *Appl. Phys. Lett.* **78**, 1487 (2001).
- ¹¹ J.-K. Hwang, S.-B. Hyun, H.-Y. Ryu, and Y.-H. Lee *J. Opt. Soc. Am. B* **15**, 2316 (1998).
- ¹² M. M. Sigalas, K. M. Ho, R. Biswas and C. M. Soukoulis, *Phys. Rev. B* **57**, 3815 (1998).
- ¹³ H. Hirayama, T. Hamano, Y. Aoyagi, *Appl. Phys. Lett.* **69**, 791 (1996).
- ¹⁴ B. Temelkuran and E. Ozbay and J. P. Kavanagh, G. Tuttle and K. M. Ho, *Appl. Phys. Lett.* **72**, 2376 (1998); B. Temelkuran, M. Bayidir and E. Ozbay and R. Biswas, M. M. Sigalas, G. Tuttle and K. M. Ho, *J. Appl. Phys.* **87**, 603 (2000).
- ¹⁵ I. Schnitzer, E. Yablonovitch, A. Scherer, and T. J. Gmitter in "Photonic Band Gaps and Localization" ed. by C. M. Soukoulis, NATO ASI SERIES B **308**, 369 (1993).
- ¹⁶ D. F. Sieven, C. F. Lam, E. Yablonovitch, *Appl. Opt.* **37**, 2074 (1998).
- ¹⁷ M. Rattier, H. Benisty, C. J. Smith, A. Beraud, D. Cassagne, C. Jouanin, T. F. Krauss and C. Weisbuch *IEEE J. Quant. Electr.* **37**, 237 (2001).
- ¹⁸ J. B. Pendry, *J. Mod. Opt.* **41**, 209 (1994).
- ¹⁹ J. B. Pendry and P. M. Bell in "Photonic Band Gap Materials" ed. by C. M. Soukoulis, NATO ASI SERIES E **315**, 203 (1996).
- ²⁰ A. Taflove, *Computational Electrodynamics - The Finite Difference Time-Domain Method* (Artech House, 1995).
- ²¹ M. Agio, E. Lidorikis and C. M. Soukoulis *J. Opt. Soc. Am. B* **17**, 2037 (2000).
- ²² Z. P. Liao, H. L. Wong, B. P. Yang, and Y. F. Yuan, *Sci. Sinica (series A)* Vol. XXVII, 1063-1076 (1984).
- ²³ P. R. Villeneuve, S. Fan and J. D. Joannopoulos and K.-Y. Lim, J. C. Chen, G.S. Petrich, L. A. Kolodziejski and R. Reif in "Photonic Band Gap Materials" ed. by C. M. Soukoulis, NATO ASI SERIES E **315**, 411 (1996).
- ²⁴ D. Labilloy, H. Benisty, C. Weisbuch, T. F. Krauss, R. M. De La Rue, V. Bardinal, R. Houdre, U. Oesterle, D. Cassagne, and C. Jouanin, *Phys. Rev. Lett.* **79**, 4147 (1997).

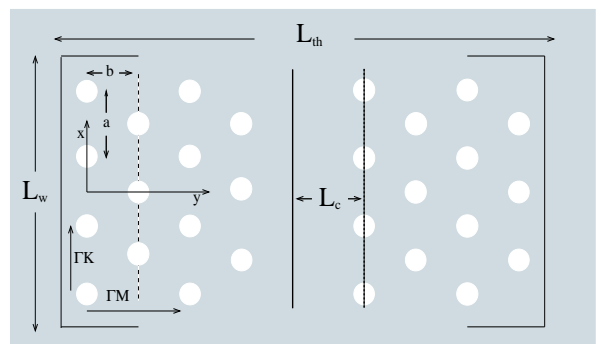


FIG. 1. The cavity structure under study. The bulk crystals symmetry directions ΓK and ΓM are shown. L_c refers to the cavity width . For the actual crystal $2b=\sqrt{3}a$ but in the TMM due to necessary approximations $2b=1.7 a$. L_w is the lateral width of the cavity while L_{th} is the thickness of the cavity system.

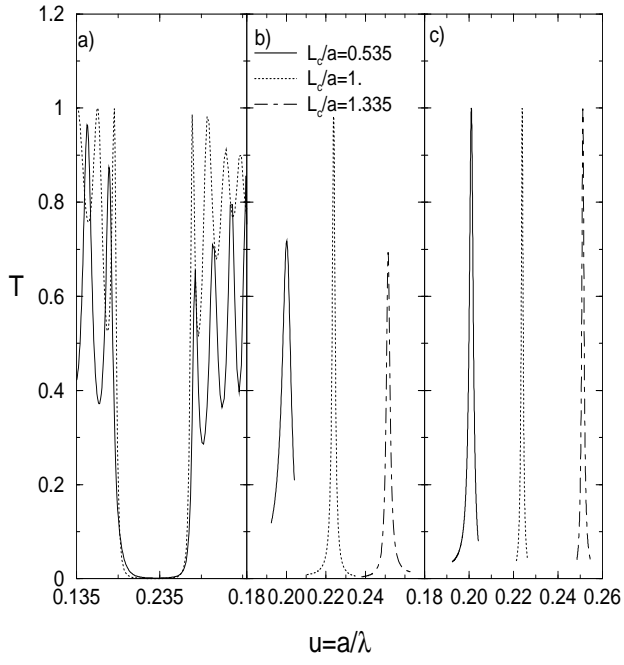


FIG. 2. a) Transmission versus reduced frequency $u=a/\lambda$ calculated with the TMM for the periodic system ($L_c = 0$). The solid lines give the results for the case of the whole structure embedded in air while the dotted line corresponds to the case of the whole structure embedded in GaAs (ϵ is taken to be 11.3). b) Resonant peaks for three values of L_c/a when the whole structure is embedded in air. The peak represented with a solid line is 1st order, the one with the dotted line is 2nd order and the one with the dot-dashed line is 3rd order. (TMM result) c) The resonant peaks for structures with the same cavity lengths L_c but being embedded in a dielectric of $\epsilon = 11.3$. (TMM result).

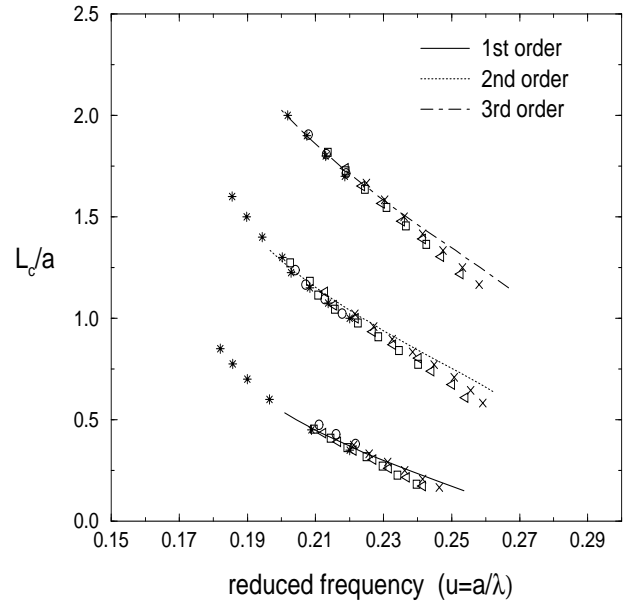


FIG. 3. The cavity width vs. the reduced frequency of the corresponding observed cavity resonant peaks. The results are obtained with the TMM (solid dotted and dot-dashed line). The experimental results for various lattice constants a are shown for comparison. The stars, circles, squares, triangles (left), x's are for $a=200, 210, 220, 230, 240$ nm respectively.

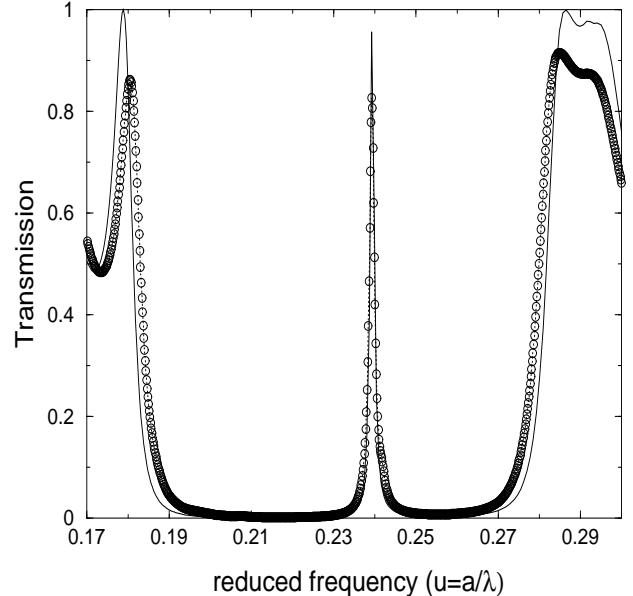


FIG. 4. Comparison between transmission results obtained with the transfer matrix technique (solid line) and the FDTD (dotted line with circles), for $L_c/a=0.85$. In order to make the comparison in this particular case we considered an approximate triangular structure ($2b=1.7a$) in the FDTD method too. The quality factor of the resonant peak in the figure is $Q \sim 211$ and $Q \sim 151$ for the TMM and FDTD result respectively.

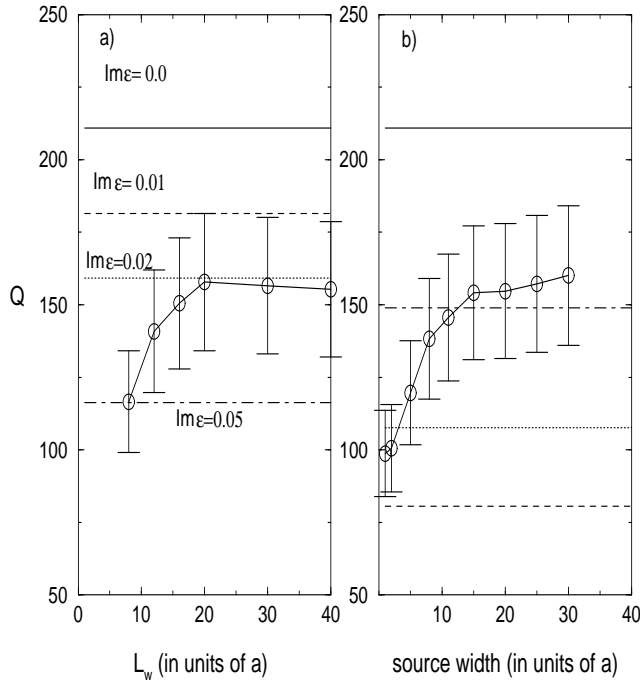


FIG. 5. a) The quality factor Q for a structure with a width $L_c/b = 1$. ($2b = \sqrt{3} a$ is taken) calculated with the FDTD versus L_w (in units of a) (see Fig. 1). The source is chosen to have length approximately half to the latteral length of the structure for all L_w . There is an error associated with the estimation of the quality factor represented by the error bars in the graph. A rough estimate is made that is expected to overestimate the actual error. The different horizontal lines correspond to values of the quality factor calculated with the TMM for the same L_c/b (but with $2b=1.7$ a) for various imaginary parts in the air dielectric constant to account for out of plane losses b) The quality factor Q calculated with the FDTD (solid line with circles) with the same L_c/b as in (a), versus the source width (in units of a). L_w is kept constant and equal to $40a$. As horizontal lines the transfer matrix results (solid line) for $L_c/b = 1$. as well as experimental results with values L_c/b close to one are also shown. The dot-dashed, dotted, and dashed and horizontal lines correspond to experimental results with $a=220$, 230 , 240 nm respectively. (Their respective L_c/b values are 0.971 , 1.004 and 1.034).

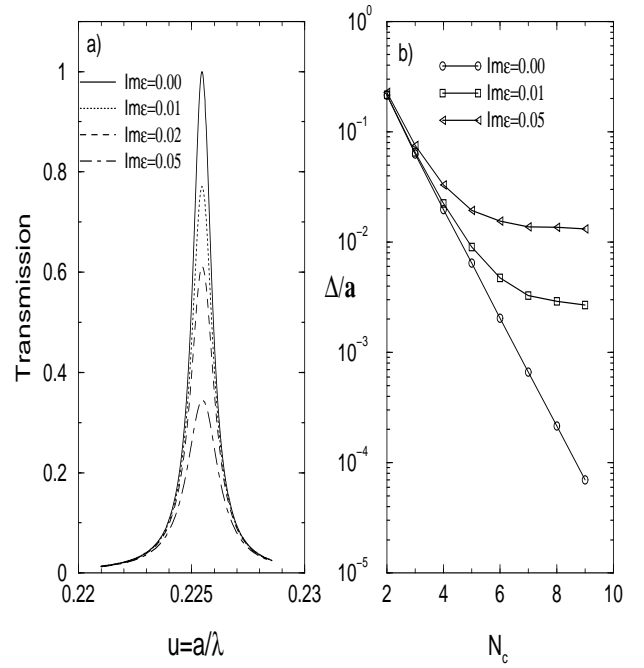


FIG. 6. a) Transmission calculated by the TMM versus reduced frequency $u=a/\lambda$ for different values of $\text{Im } \epsilon$ of the air dielectric. $L_c/a = 0.985$ on the cavity resonance (for $N_c = 4$). b) The dimensionless linewidth (Δ is $\delta\lambda$ i.e. the wavelength width that corresponds to transmission half of the peak's maximum) vs. N_c (number of rows in each side of the cavity) for the lossless case as well as the cases with non-zero imaginary part in the air dielectric constant.

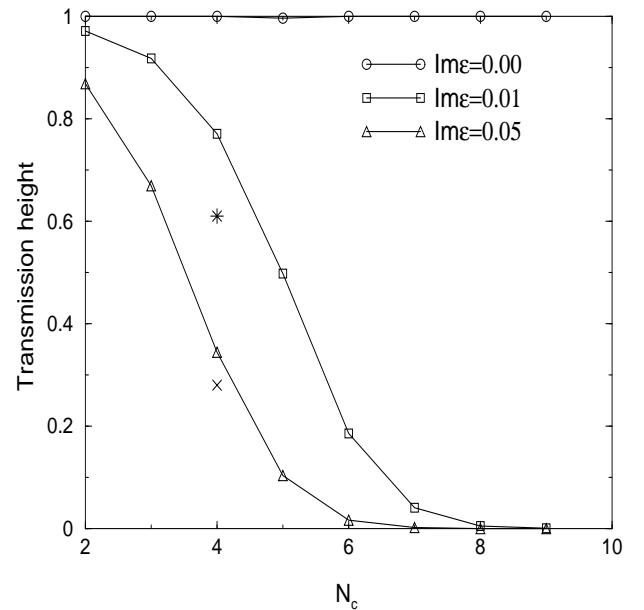


FIG. 7. The Transmission height of the resonance for $L_c/a=0.985$ for three values of the imaginary part of the air dielectric constant, $\text{Im } \epsilon$. Two experimental values for the cavity with $N_c=4$ are shown for comparison. The star and ex correspond to $a=200$ nm with $L_c/a=0.9815$ and $a=220$ nm with $L_c/a=0.9709$ respectively.

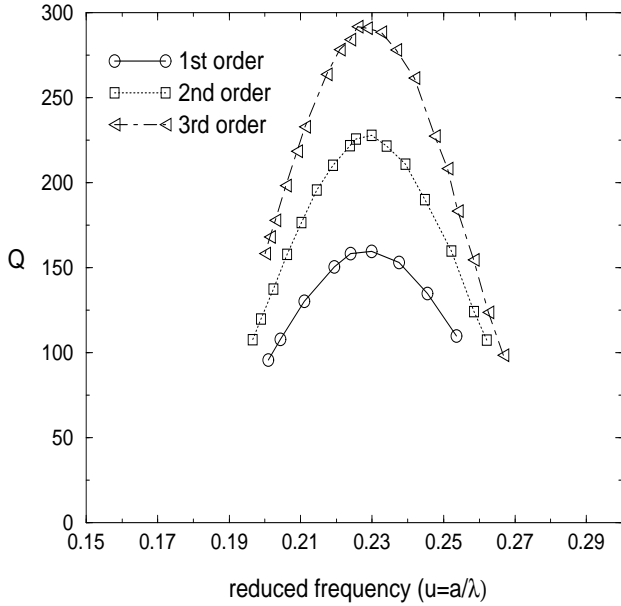


FIG. 8. The quality factor calculated with the TMM versus the reduced frequency for 1st 2nd and 3rd order resonant peaks.

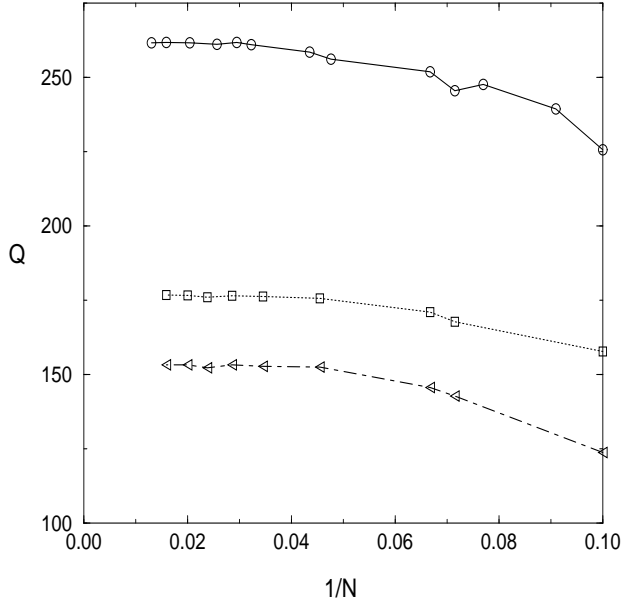


FIG. 9. The quality factor for three different cavity peaks with reduced frequencies $u=0.2255$ (solid line), $u=0.2063$ (dotted line) and $u=0.2628$ (dotted-dashed line) vs. $1/N$ where N is the number of grid spacings that the lattice constant a is divided into in the computation. The peaks at $u=0.2255$ and $u=0.2063$ are second order peaks and have $L_c/a=0.985$ and $L_c/a=1.2$ respectively. The peak at $u=0.2628$ is of third order (with $L_c/a=1.2$). The quality factor saturates at a value as the numerical accuracy of the method increases.

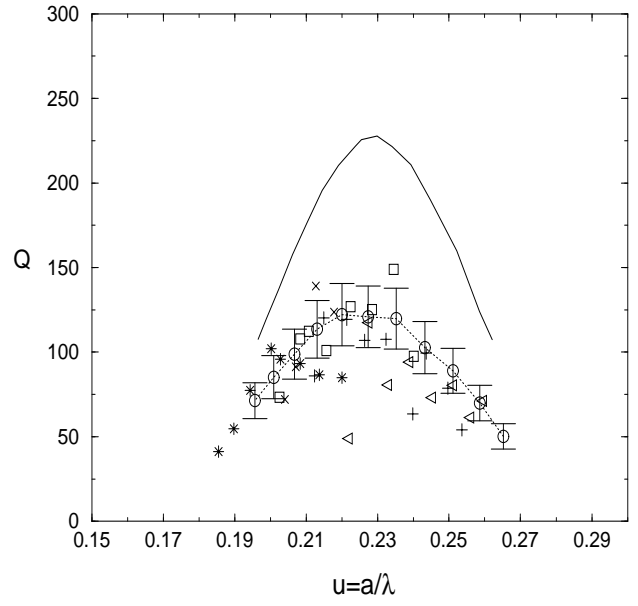


FIG. 10. The quality factor vs. the reduced frequency for 2nd order peaks calculated with the TMM (solid line) and FDTD method (dotted line with circles). The error bars in the FDTD method are a rough estimate. In the FDTD $L_w=40a$ and a source with width equal to $5a$ is used. Experimental 2nd order cavity peaks for various lattice constants a are also plotted to be seen in comparison with the two calculational methods. The star, ex, square, plus and trialgle (left) correspond to $a=200, 210, 220, 230, 240$ nm respectively.